AWARD NUMBER:	W81XWH-20-1-0094
TITLE:	Prognostic selection of osteogenic stem cells using label-free microfluidic separation
PRINCIPAL INVESTIGATOR:	Quanjun Cui, MD.
CONTRACTING ORGANIZATION:	University of Virginia, Charlottesville, VA
REPORT DATE:	March 2021
TYPE OF REPORT:	Annual Report
PREPARED FOR:	U.S. Army Medical Research and Development Command Fort Detrick, Maryland 21702-5012
DISTRIBUTION STATEMENT:	Approved for Public Release; Distribution Unlimited

REPORT DOCUMENTATION PAGE

Form Approved
OMB No. 0704-0188

1. REPORT DATE	2. REPORT TYPE	3. DATES COVERED
March 2021	**Annual Report**	**01Feb2020-31Jan2021**

4. TITLE AND SUBTITLE

Prognostic selection of osteogenic stem cells using label-free microfluidic separation

5a. CONTRACT NUMBER
W81XWH2010094

5b. GRANT NUMBER
W81XWH-20-1-0094

5c. PROGRAM ELEMENT NUMBER

6. AUTHOR(S)
Quanjun Cui, MD; Nathan Swami, PhD; Abhijit S. Dighe, PhD

E-Mail: QC4Q@hscmail.mcc.virginia.edu

5d. PROJECT NUMBER

5e. TASK NUMBER

5f. WORK UNIT NUMBER

7. PERFORMING ORGANIZATION NAME(S) AND ADDRESS(ES)

The Rector and Visitors of the University of Virginia
PO Box 400195
Charlottesville, VA 22904-4195

8. PERFORMING ORGANIZATION REPORT NUMBER

9. SPONSORING / MONITORING AGENCY NAME(S) AND ADDRESS(ES)

U.S. Army Medical Research and Development Command
Fort Detrick, Maryland 21702-5012

10. SPONSOR/MONITOR'S ACRONYM(S)
PRMRP

11. SPONSOR/MONITOR'S REPORT NUMBER(S)

12. DISTRIBUTION / AVAILABILITY STATEMENT

Approved for Public Release; Distribution Unlimited

13. SUPPLEMENTARY NOTES

14. ABSTRACT

Our central hypothesis is that while mixed adipose derived stem cells (ADSCs) fail to induce bone formation, the smallest sized ADSCs with the least granularity, that can be isolated in a pure form using microfluidic separation, will induce bone formation reliably and consistently. We seek to develop a label-free, high-throughput, microfluidic isolation platform for the isolation of adipose derived stem cells (ADSCs), without the need for surface markers. In the period under report, we have compared biophysical characteristics of a bone forming (positive control) stem cells population with mixed ADSCs and based on that we have successfully devised microfluidic platform to isolate the sub-population of ADSCs that will possess reliable bone-forming potential.

15. SUBJECT TERMS

16. SECURITY CLASSIFICATION OF:			17. LIMITATION OF ABSTRACT	18. NUMBER OF PAGES	19a. NAME OF RESPONSIBLE PERSON
a. REPORT	b. ABSTRACT	c. THIS PAGE			USAMRMC/
Unclassified	Unclassified	Unclassified	Unclassified	10	19b. TELEPHONE NUMBER *(include area code)*

TABLE OF CONTENTS

Specific aims:

Aim 1 will optimize the microfluidic platform for isolation of the osteogenic population of ADSCs from Balb/c derived mixed ADSCs. **Aim 2** will determine distribution of predictive markers for osteogenic MSCS (CDAM1) in different ADSCs population.

Introduction:

A significant percentage (up to 20 %) of the 7.9 million fractures that occur annually in the United States can fail to heal due to development of non-unions, thereby requiring surgical intervention.[1]. Therapeutic delivery of bone-marrow derived mesenchymal stem cells (MSCs) has shown promising results in clinical trials of fracture repair.[2] However, isolation of these cells from a donor is invasive and typically very low numbers of MSCs can be obtained from bone marrow aspirate [2]. Alternatively, ADSCs that have a higher proliferative capacity, frequency of occurrence (500 X more), and ability to retain their differentiation potential for longer period than MSCs can be isolated using a simple procedure (e.g. needle aspiration of fat)[3]. However, unpurified ADSCs have shown poor osteogenic potential *in vivo* and are not able to facilitate bone regeneration.
Bone morphogenetic proteins (BMPs) play an important role in the development of bone and cartilage, and has been shown to induce both osteogenic differentiation *in vitro* and bone formation *in vivo* [4]. Our team has previously shown that FACS-purified CD105+CD34- ADSCs maximally responded to BMPs *in vitro* but failed to induce any bone formation *in vivo* [5]. On the other hand, a clonally purified, bone marrow derived, osteoprogenitor population of the phenotype $CD105^{-}CD34^{-}$ did not respond to BMPs *in vitro* but showed robust bone formation following subcutaneous implantation on a scaffold in Balb/c mice. CD105 and CD34 linked BMP-responsiveness and associated bone forming ability warrants further examination. Since we had not tested bone forming ability of CD105-CD34- ADSCs and the use of FACS-purified stem cells will not meet FDA requirement of minimal manipulation, this project seeks to characterize the differences between CD 105^{-} and CD 105^{+} phenotypes of ADSCs, using label-free microfluidic separation. We postulate that CD105- ADSCs will be bone forming sub-population of ADSCs and it is feasible to purify this sub-population using label-free size-based microfluidic separation methods.

Keywords: Adipose derived stem cells (ADSCs), CD105, microfluidic, impedance cytometry, Deterministic lateral displacement (DLD)

Accomplishments

1. Comparing unsorted ADSCs with D1 MSCs using flow cytometry and labelled monoclonal antibodies for CD105 and CD34

D1 cells were purchased from ATCC and cultured and maintained in DMEM medium. ADSCs were isolated from 8 weeks old, female, Balb/c mice. ADSCs were grown in DMEM medium and large stock of ADSCs was prepared as the master stock for future experiments which was stored in liquid nitrogen. All the experiments were performed using passage 3 or 4 (P3 or P4) ADSCs. D1 cells and ADSCs were stained with anti-C105 and anti-CD34 antibodies and analyzed using a flow cytometer. The data clearly showed that ADSCs present a $CD105^{+}$ and a CD105- sub-population (Fig. 1 a-c), while D1 cells show negative expression of CD34 and CD105 (Fig. 1 d-f).

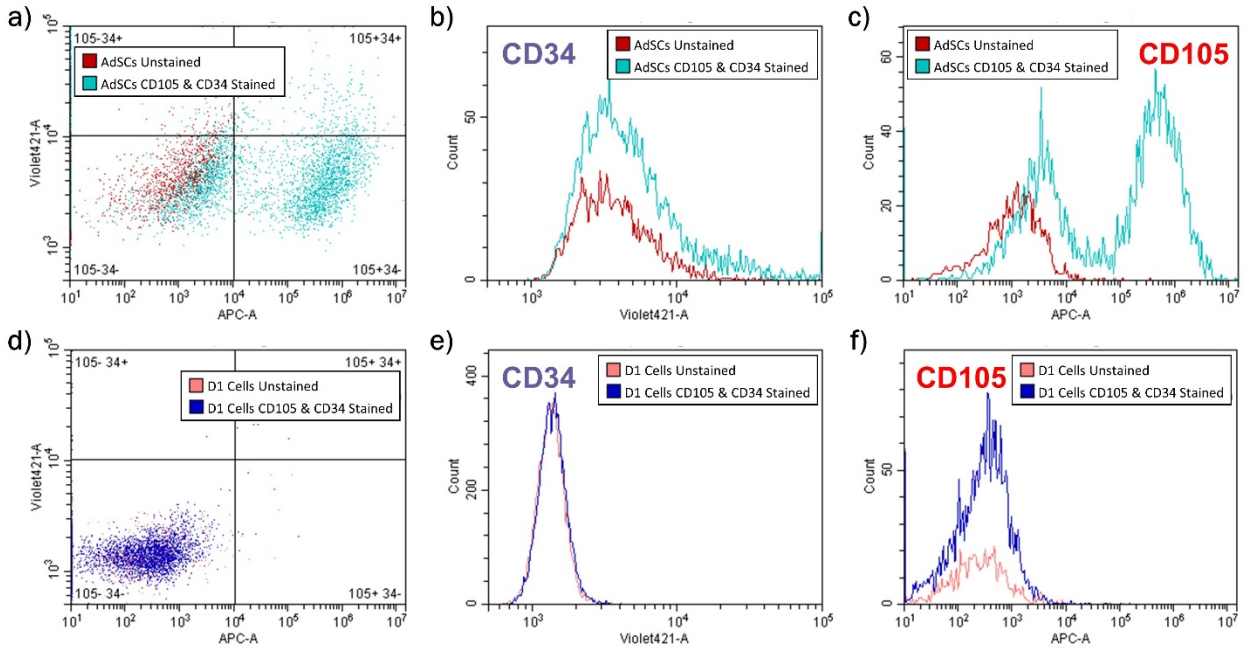

Figure 1 – Flow cytometry of (**a-c**) adipose-derived stem cells (ADSCs) and (**d-f**) D1 cells for samples stained with CD34 (Violet421 filter) and CD105 (APC filter). Scatter plots of CD105 (APC) *versus* CD34 (Violet421) for **a)** ADSCs and **d)** D1 cells. Histograms for fluorescence expression of CD34 (**b, e**) and CD105 (**c, f**) for ADSCs (**b, c**) and D1 cells (**e, f**).

Comparison between ADSCs and D1 cells by flow cytometry (**Figure 2a**) also shows that there are size (**Figure 2b**) and internal composition (**Figure 2c**) differences between the two stem cells populations, as assessed by forward scatter (FSC) and side scatter (SSC), respectively. Specifically, bone-forming D1 cells are smaller than ADSCs, with the latter presenting a broader distribution in size.

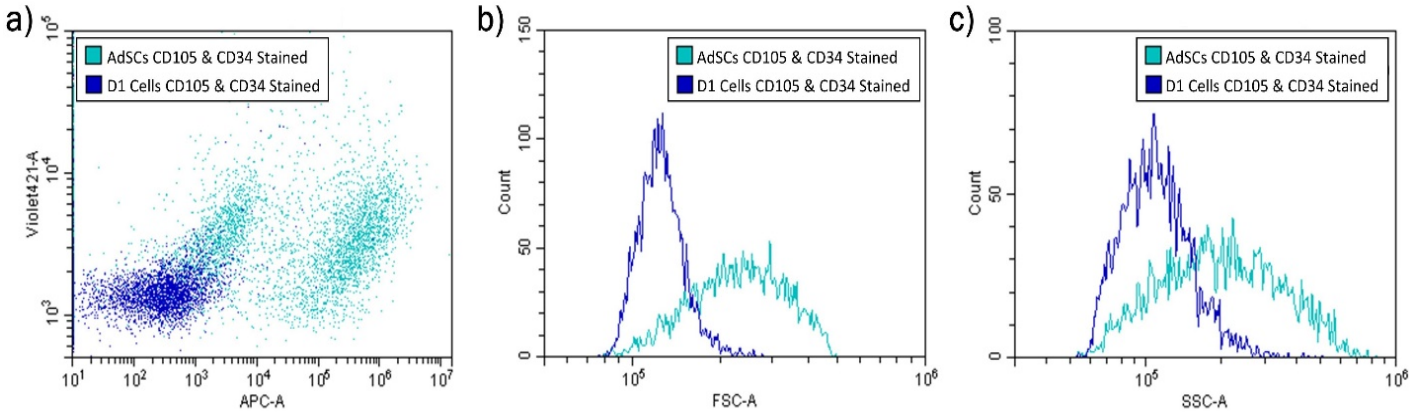

Figure 2 – Flow cytometry of ADSCs and D1 cells for samples stained with CD34 (Violet421) and CD105 (APC). **a)** Scatter plot of CD105 (APC) *versus* CD34 (Violet421) for ADSCs and D1 cells. Histograms for **b)** forward scatter (FSC) and **c)** side scatter (SSC) for ADSCs and D1 cells.

2. Comparing unsorted ADSCs with D1 MSCs using impedance cytometry

To evaluate the feasibility of purifying CD105+ and CD105- sub-populations of ADSCs using microfluidics platform, we first investigated the biophysical characteristics of the stem cells populations. ADSCs and D1 cells were characterized by impedance cytometry (**Figure 3**). Data was analyzed in terms of the biophysical metrics of electrical diameter and ϕZ Contrast, which provides information about singe-cell size and interior complexity, respectively. Results showed that ADSCs were significantly ($*p = 0.0175$) larger (16.7 ± 6.88 μm) and had a broader distribution (CV = 0.41) than D1 cells (13.7 ± 2.83 μm; CV = 0.21) – **Figure 3c,d**. Moreover, there are significant ($*p = 0.0454$) differences in the interior properties of ADSCs and D1 cells (**Figure 3e**).

Since the CD105$^-$ D1 cells presented a higher bone-forming potential in prior work, the size-overlap of the smaller ADSCs with the size distribution of the bone-forming D1 cells, suggests that a size-based enrichment method could be of interest.

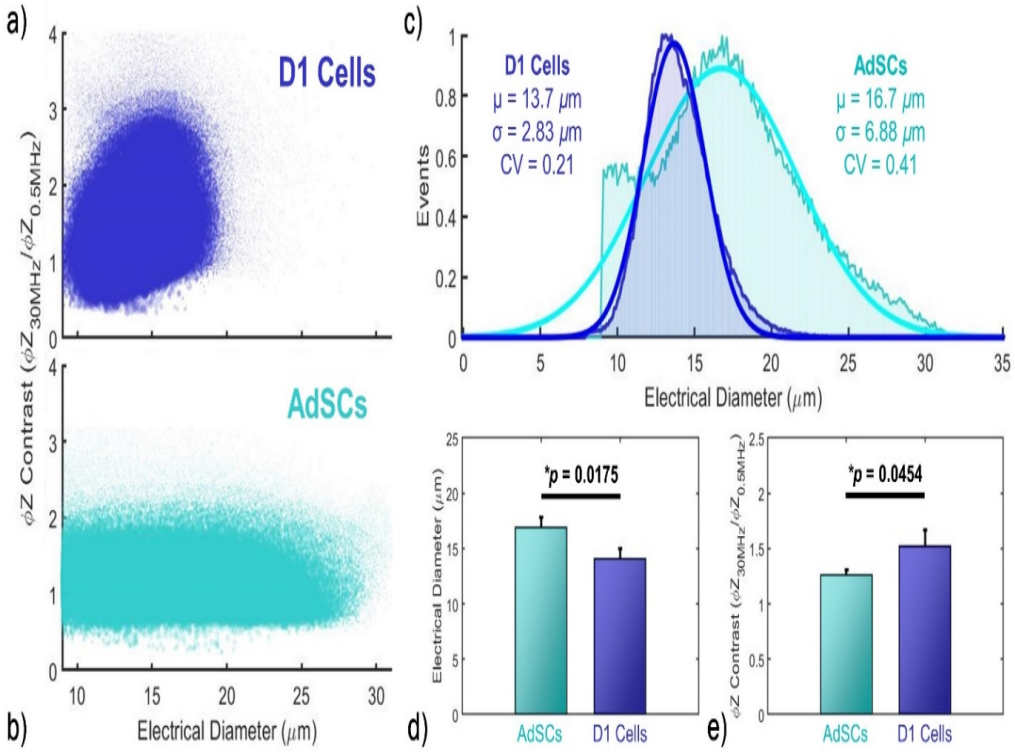

Figure 3 – Impedance cytometry of ADSCs and D1 cells. Scatter plots of particle electrical diameter (estimated using Impedance Magnitude (|Z|) at 500 kHz) *versus* Impedance Phase (ϕZ) Contrast, calculated as the ratio of high frequency phase (30 MHz) over low frequency phase (500 kHz) of **a)** D1 cells and **b)** ADSCs. **c)** Normalized histograms of electrical diameter for ADSCs and D1 cells together with Gaussian distributions fits to the data. Bar plots comparing ADSCs and D1 cells for **c)** electrical diameter and **e)** ϕZ contrast. Data represent between 100,000 to 200,000 events from $n = 3$ biological repeats; statistical significance: $*p \leq 0.05$.

3. Purification and characterization of CD105$^+$ and CD105$^-$ ADSCs

While the prior section confirms that the smaller sized ADSCs overlap with bone-forming D1 MSCs, we seek to understand the size differences of the CD105$^+$ and CD105$^-$ fractions of the ADSCs, since the latter ADSCs

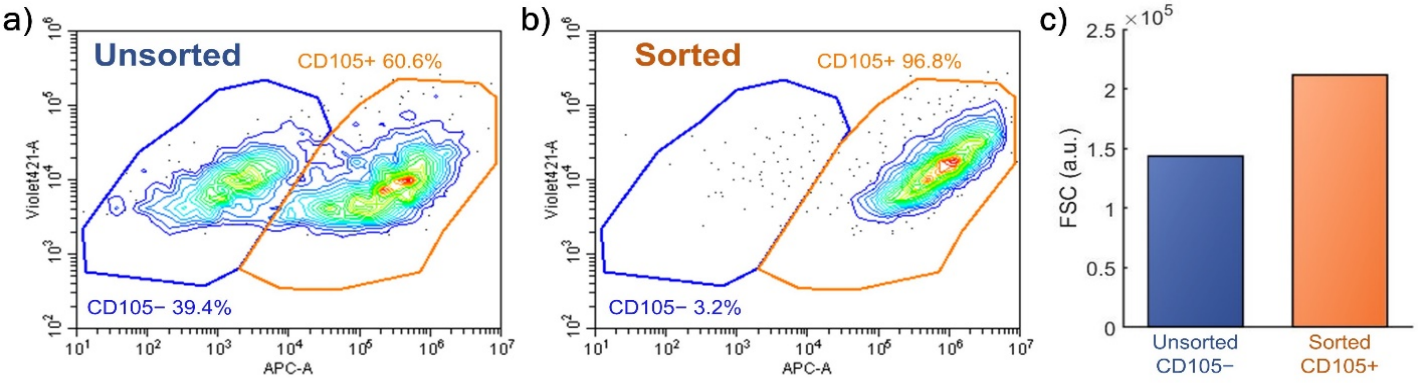

fraction is hypothesized to exhibit bone-forming properties *in vivo*. For this purpose, we used a magnetic sorting

Figure 4 – Flow cytometry of (**a-c**) adipose-derived stem cells (ADSCs) and (**d-f**) D1 cells for samples stained with CD34 (Violet421 filter) and CD105 (APC filter). Scatter plots of CD105 (APC) *versus* CD34 (Violet421) for **a)** ADSCs and **d)** D1 cells. Histograms for fluorescence expression of CD34 (**b, e**) and CD105 (**c,f**) for ADSCs (**b, c**) and D1 cells (**e, f**).

step utilizing antibody conjugated beads, to enrich the $CD105^+$ ADSCs sub-population from the $CD105^-$ fractions. Flow cytometry results (**Figure 4a, b**) confirmed that the enrichment step was successful at enriching $CD105^+$ cells, with the ratio of $CD105^-$ to $CD105^+$ going from ~39% to 61% in the unpurified sample to ~3% to 97% in the sorted sample. Analysis of the mean size of cells based on the FSC data (**Figure 4c**) showed that unsorted
$CD105^-$ were indeed smaller than sorted $CD105^+$ ADSCs. This reinforces the notion that a size-based enrichment technique could be implemented to retrieve the $CD105^-$ fraction, that is expected to show superior osteogenic potential, from a heterogeneous ADSCs population.

4. Label-free size-selective sorting of ADSCs

The observations presented so far suggest that a size-based selection method for smaller ADSCs can potentially enrich the $CD105^-$ subpopulation that is expected to show superior bone-forming capabilities *in vivo*. Deterministic lateral displacement, or DLD, is a label-free, size-based particle sorting technique that could be ideal for this situation[6]. In this technique, sorting is deterministically decided by the design of an array of posts throughout the device. Particles smaller than a critical size (D_C) follow the continuous flow direction (in a "zig-zag mode"), while larger particles are laterally displaced (in a "displacement mode") and move in a direction predefined by the array (**Figure 5a**).

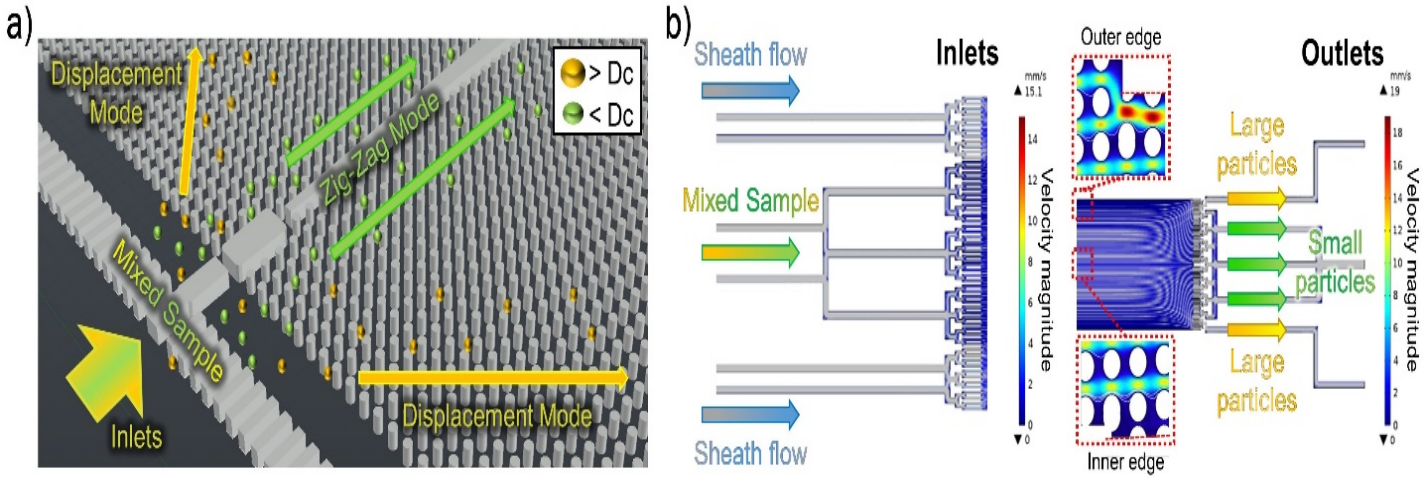

Figure 5 – **a**) Deterministic lateral displacement (DLD) operation principle. Particles larger or smaller than a critical size (D_C) displace diagonally (displacement mode) or follow flow streamlines (zig-zag mode), respectively. **b)** Computational Fluid Dynamics (CFD) simulations for designing separation device inlets, outlets and post array edges to balance hydrodynamic resistances.

The occurrence of these two modes is defined by the geometrical parameters of the post array, i.e., the critical size D_C is defined by an interplay between post diameter, lateral gap between posts, distance between post-centers and the consecutive lateral shifting of rows of posts within the array. This lateral shift divides the flow-stream into parallel streamlines along the array, and particles are forced to either follow the central streamline ("zig-zag") or consecutively change streamlines laterally ("displacement") according to the predefined D_C. However, this behavior is pinned on a proper distribution of the hydrodynamic resistance across the post array.

To confirm this, CFD simulations were performed to ensure correct balancing of resistances across the device (**Figure 5b**). At the Inlets region, resistance must be balanced so that particles enter the device in the correct location and are kept focused at its center using side sheath-flow lanes. This guarantees that only larger particles are displaced outwardly and move into the sheath-flow lanes, while keeping smaller particles focused at the device center. At the Outlet region, resistance must be balanced so that particles exit the device in the correct lanes, so that there is no cross-contamination of particles between the outlet channels for larger and smaller particles. Finally, the edges of the array must also be optimized so that the hydrodynamic resistance is kept

balanced at these critical positions and the streamlines are kept constant throughout the whole width of the post array[7].

Based on this, devices to remove the larger ADSCs from the sample were designed, with the first iterations having D_C values of 9.58, 10.45 and 11.63 μm. These D_C values were selected mostly for preliminary testing of the experimental conditions that will be later used in in ADSCs separations. A first run was performed using a DLD device of D_C = 9.58 μm and a mixture of 7 μm and 12 μm polystyrene beads (**Figure 6a**). The mixed sample enters the device at the center region with sheath flow keeping the sample focused (**Figure 5 & 6a**). Thus, larger particles than the defined D_C will be displaced outwardly and collected at outer outlets (**Figure 5b & 6a**). Counting of single beads by flow cytometry showed (**Figure 6b**) that while the mixed sample at the inlet had an approx. 60:40 % ratio of 7 to 12 μm beads, the ratio is changed to approx. 20:80 % at the large particles outlets, proving the effective removal of larger particles from the main population.

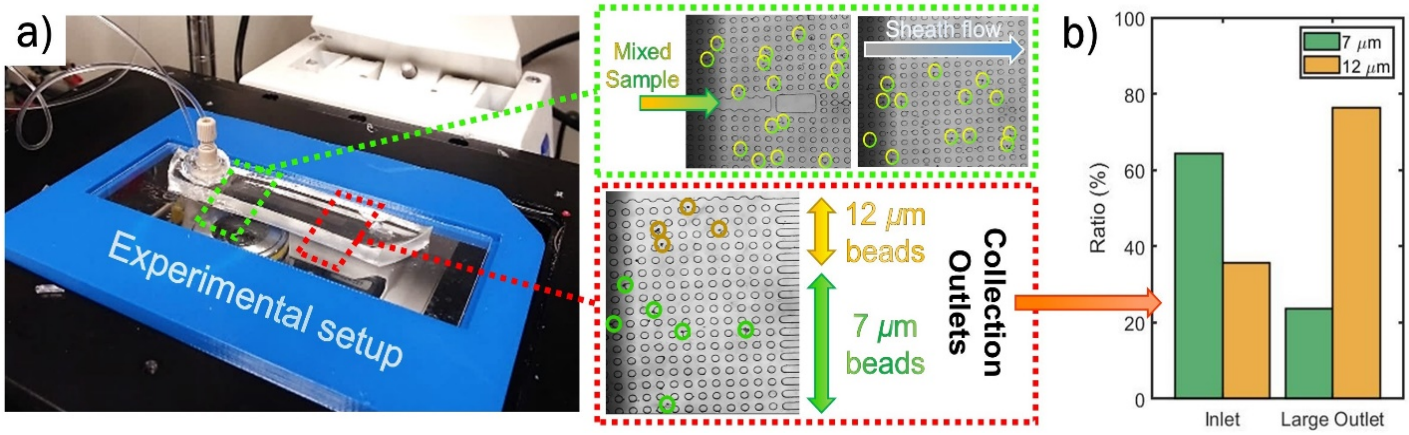

Figure 6 – **a**) Experimental setup of the DLD device in a custom 3D-printed holder. Inserts show the central entrance area of the device with a mixed sample, the outer area of the device with sheath flow keeping particles focused, and the outlet region, with large and small particles aligned with their respective outlet channels. **b)** Separation of 7 μm and 12 μm polystyrene beads as assessed by flow cytometry. Population ratios for the Inlet and Larger Outlet fractions show the removal of larger particles from the original mixture sample.

Impact:

We have shown that bone-forming CD105- D1 cells exhibit small sizes and developed a microfluidic platform utilizing the DLD principle that can be used for size-based separation to isolate CD105- ADSCs from primary, mixed, population of ADSCs. Our initial runs suggest the ability to isolate 10,000-50,000 purified, CD105- ADSCs over a 30-minute collection time. We are working to control over the size-selectivity of the collected fraction for differentiating sub-populations that have size differences in the ≤5 μm. This device can also potentially separate and analyze the size fractions of the collected phenotype at the outlet of the same chip, without having to stain and do flow cytometry off-chip. These are the significant milestones achieved in the first year of this project.

Future work:

In the upcoming year, we will undertake the following tasks:

(1) Surface markers on size-selected ADSCs: We will focus on improving collection efficiency by improving microfabrication of device molds, since these affect definition of posts and resistance balancing across the device array. We will also optimize the collection process, since this can affect the accurate characterization of sorting efficiency by flow cytometry. Based on this, we will develop protocols for sorting ADSCs into bins <15 μm, <12 μm and <10 μm, so that we can stain and measure the distribution of CD expression by flow cytometry.

(2) Size distribution of FACS sorted ADSCs: Analogous with the above task, we will utilize FACS-purified ADSCs to enable studies with homogeneous fractions of $CD105^-$ and $CD105^+$ to obtain an improved understanding of the size distribution of each sample type, which can be used to optimize the D_C values of DLD devices.
(3) *In vitro* osteogenic differentiation abilities of separated ADSCs fractions: The fractions obtained in task #1 and #2 will be investigated *in vitro* for their ability to differentiate into osteogenic lineage. The cells will be grown for 21 days and stained using alizarin red at days 7, 14, 21 to quantitatively determine mineralization. Osteogenic differentiation will also be determined using alizarin red staining, ALP activity and gene expression of osteogenic markers (RunX2, Osterix, Dlx5, Msx2, Col I, OCN, BSP and ALP). The BMP-responsiveness of parental stem cells population as well as purified sub-populations will be assessed by adding 100 ng BMP-2 to the medium.
The stem cells populations will be stained for CD105, CD34, CD146 and CADM1. CD146 and CADM1 are predictive markers for the stem cells to forecast their superior osteogenic potential. We will determine whether microfluidics-purified stem cells display enhanced expression of these receptors. This test can then be utilized for quality control purposes.
(4) *In vivo* bone forming abilities of separated ADSCs fractions: The stem cells populations, parental ADSCs as well as microfluidic device purified sub-populations will be subjected to evaluation for their bone forming ability, in comparison with control D1 cells group. ADSCs, purified stem cells and bone-forming control D1 cells will be cultured for 7 days *in vitro*. After 7 days, cells will be mixed with matrigel and then will be implanted into sub-cutaneous tissues of the Balb/c mice. The bone formation will be determined using radiography, MicroCT, histology and real time PCR after 8 and 12 weeks.

Changes/Problems

There were several problems associated with the pandemic and associated restrictions imposed by our institution – hiring freeze, restrictions on vivarium usage, traffic between medical school and engineering school was not freely allowed, only select few students and staff were allowed on the campus; to site a few examples. Although this took a toll on the project, we managed to fulfill the tasks with the help of existing post docs and students in our groups.

As for the science, we did make one change in the plan. We had originally proposed to use inertial separation to devise a microfluidic platform for isolation of CD105- ADSCs. However, as explained in the accomplishments section, we found that the size differences of sub-population of ADSCs were not enough to use this approach. Therefore, we used deterministic lateral displacement which can handle very small size differences.

Products

None.

Participants & Other Collaborating Organizations

Quanjun Cui, (Principal Investigator)
Nathan Swami, (Co-Investigator)
Abhijit S. Dighe (Co-investigator)
Farzana Liakath (Post doc)
Gina Beck (Research Specialist)
John Moore (Graduate Student)
Carlos Honrado (Post doc)

8. Special Reporting Requirements

None.

9. Appendices

References:

[1] Aspenberg, P.; Genant, H. K.; Johansson, T.; Nino, A. J.; See, K.; Krohn, K.; García-Hernández, P. A.; Recknor, C. P.; Einhorn, T. A.; Dalsky, G. P.; Mitlak, B. H.; Fierlinger, A.; Lakshmanan, M. C., Teriparatide for acceleration of fracture repair in humans: a prospective, randomized, double-blind study of 102 postmenopausal women with distal radial fractures. *Journal of bone and mineral research : the official journal of the American Society for Bone and Mineral Research* **2010,** *25* (2), 404-14.

[2] Hernigou, P.; Poignard, A.; Beaujean, F.; Rouard, H., Percutaneous autologous bone-marrow grafting for nonunions. Influence of the number and concentration of progenitor cells. *The Journal of bone and joint surgery. American volume* **2005,** *87* (7), 1430-7.

[3] Strioga, M.; Viswanathan, S.; Darinskas, A.; Slaby, O.; Michalek, J., Same or not the same? Comparison of adipose tissue-derived versus bone marrow-derived mesenchymal stem and stromal cells. *Stem cells and development* **2012,** *21* (14), 2724-52.

[4] Chen, D.; Zhao, M.; Mundy, G. R., Bone morphogenetic proteins. *Growth factors (Chur, Switzerland)* **2004,** *22* (4), 233-41.

[5] Madhu, V.; Kilanski, A.; Reghu, N.; Dighe, A. S.; Cui, Q., Expression of CD105 and CD34 receptors controls BMP-induced in vitro mineralization of mouse adipose-derived stem cells but does not predict their in vivo bone-forming potential. *Journal of Orthopaedic Research* **2015,** *33* (5), 625-632.

[6] McGrath J, Jimenez M, Bridle H. Deterministic lateral displacement for particle separation: a review. *Lab on a Chip*. **2014**; 14(21):4139-58.

[7] Inglis DW. Efficient microfluidic particle separation arrays. *Applied Physics Letters*. **2009**; 94 (1) : 013510.